PHYSICAL REVIEW E **83**, 050602(R) (2011)

First-order layering and critical wetting transitions in nonadditive hard-sphere mixtures

Paul Hopkins[1] and Matthias Schmidt[1,2]

[1]*H. H. Wills Physics Laboratory, University of Bristol, Tyndall Avenue, Bristol BS8 1TL, United Kingdom*

[2]*Theoretische Physik II, Physikalisches Institut, Universität Bayreuth, D-95440 Bayreuth, Germany*

(Received 17 January 2011; published 31 May 2011)

Using fundamental-measure density functional theory we investigate entropic wetting in an asymmetric binary mixture of hard spheres with positive nonadditivity. We consider a general planar hard wall, where preferential adsorption is induced by a difference in closest approach of the different species and the wall. Close to bulk fluid-fluid coexistence, the phase rich in the minority component adsorbs either through a series of first-order layering transitions, where an increasing number of liquid layers adsorbs sequentially, or via a critical wetting transition, where a thick film grows continuously.

DOI: 10.1103/PhysRevE.83.050602 PACS number(s): 68.08.Bc, 82.70.Dd, 64.70.Ja

Studying the interfacial properties of liquid mixtures is of significant fundamental and technological relevance [1]. Bulk liquid-liquid phase separation, which can arise at or close to room temperature, is usually associated with rich phenomenology of interfacial behavior at a substrate. Gaining a systematic understanding of how the different types of intermolecular and of substrate-molecule interactions induce phenomena such as wetting, layering, and drying at substrates constitutes a major theoretical challenge. Relevant for surface adsorption of liquids are Coulombic and dispersion forces, but also solvent-mediated and depletion interactions which occur in complex liquids. Arguably the most important source for the emergence of structure in dense liquids is the short-ranged repulsion between the constituent particles; this may stem from the overlap of the outer electron shells in molecular systems or from screened charges or steric stabilization in colloidal dispersions.

Hard sphere fluids form invaluable reference models for investigating the behavior of liquids at substrates. Both the pure [2,3] and binary [4] hard sphere fluids are relevant, the latter playing an important role when adding, e.g., electrostatic interactions in order to study wetting of ionic liquids at a substrate [5]. The most general binary mixture is characterized by independent hard core distances between all different pairs of species, and is referred to the nonadditive hard sphere (NAHS) model. Here the cross-species interaction distance can be smaller or larger than the arithmetic mean of the like-species diameters. The NAHS model gives a simplified representation of more realistic pair potentials, i.e., charge renormalization effects in ionic mixtures in an explicit solvent induce nonadditive effective interactions between the ions [6]. It is also a reference model to which attractive or repulsive tails can be added [7]. The Asakura-Oosawa-Vrij (AOV) model of colloids and nonadsorbing polymers [8] is a special case where one of the diameters (that of the polymers) vanishes.

It is surprising that the wetting behavior of the general NAHS model is largely unknown, given the fundamental status of the model. In this Rapid Communication we address this problem and consider the NAHS fluid at a general, nonadditive hard wall. We find a rich phenomenology of interfacial phase transition, including two distinct types of surface transition: one is layering, where the adsorption of one of the phases occurs through a number of abrupt jumps, and the other is critical wetting, where the thickness of the adsorbed film grows continuously when varying the state point along the bulk fluid-fluid binodal. Via changing the wall properties, a crossover between these transitions occurs.

The binary NAHS model is defined by the pair potentials $v_{ij}(r) = \infty$ for $r < \sigma_{ij}$ and 0 otherwise, where $i,j = s,b$ refers to the small and big species, respectively, σ_{ss} and σ_{bb} are the diameters of the small and big particles, respectively, and r is the center-to-center distance. The cross-species diameter is $\sigma_{sb} = \frac{1}{2}(1+\Delta)(\sigma_{ss}+\sigma_{bb})$, where $\Delta \geqslant -1$ measures the degree of nonadditivity; see Fig. 1(a) for an illustration of the length scales. The model is characterized by the size ratio $q = \sigma_{ss}/\sigma_{bb} \leqslant 1$, and by Δ. In this Rapid Communication we restrict ourselves to the asymmetric size ratio $q = 0.5$, and to positive nonadditivity $\Delta = 0.2$, as a representative case. We relate Δ to a length scale via $d = \frac{1}{2}(\sigma_{ss}+\sigma_{bb})\Delta \equiv \sigma_{sb} - \frac{1}{2}(\sigma_{ss}+\sigma_{bb})$, where here $d = 0.3\sigma_{ss}$. The state point is characterized by two partial bulk packing fractions $\eta_i = \pi\sigma_{ii}^3\rho_i/6$, where ρ_i is the number density of species i. We define a general planar hard wall via the external potentials $u_i(z) = \infty$ if $z < l_i$, and 0 otherwise; here z is the distance between the wall and the particle center, and l_i is the minimal distance of approach of species $i = s,b$. Clearly the origin in z is irrelevant, so the only further control parameter is the wall offset $\delta l = l_b - l_s$. For additive hard sphere mixtures it is common to set $l_i = \sigma_{ii}/2$; for our model parameters this results in $\delta l = 0.5\sigma_{ss}$. Besides this "additive wall," two further special cases are shown in Fig. 1(b). The b-type wall has properties similar to the big particles so that it experiences these with their "intrinsic" size $l_b = \sigma_{bb}/2$, but experiences the small particles with their "nonadditive" size $l_s = \sigma_{ss}/2 + d$, such that $\delta l = 0.2\sigma_{ss}$. We expect that the bigger particles adsorb more strongly to this wall. Conversely, the s-type wall has properties similar to the small particles, so that it experiences these with their intrinsic size $l_s = \sigma_{ss}/2$, and experiences the big particles with their nonadditive size $l_b = \sigma_{bb}/2 + d$, so that $\delta l = 0.8\sigma_{ss}$. Thus, one expects the small particles to adsorb more strongly.

We investigate the inhomogeneous NAHS fluid using a fundamental-measure density functional theory [9,10]. Comparison of theoretical results to Monte Carlo simulation data for bulk fluid-fluid phase diagrams [9,10], partial radial distribution functions [9,11], and density profiles in planar slits [12] indicates very good quantitative agreement. We obtain equilibrium density distributions $\rho_i(z)$ from the grand potential

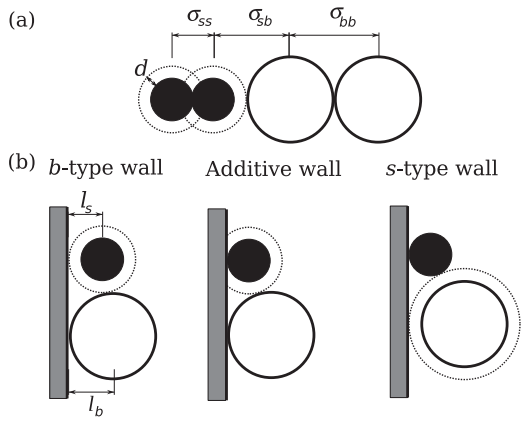

FIG. 1. (a) Illustration of the asymmetric NAHS model with positive nonadditivity. The solid boundaries represent the hard cores of the small and big species. The dotted line represents the nonadditive hard core between unlike species, which here is attributed only to smaller particles. (b) Three examples of general planar hard walls. The additive wall treats the two species equally, while the b-type and s-type walls have properties similar to the big and small particles, respectively.

functional $\Omega[\rho_s,\rho_b]$ by numerical solution of $\delta\Omega/\delta\rho_i(z) = 0$, $i = s,b$. To calculate coexisting (bulk or surface) states we use the equality of the chemical potentials μ_s, μ_b, and Ω in the two phases. The NAHS functional [9] features both a large number of terms and a large number of convolutions that take account of the nonlocality. Therefore the accurate calculation of density profiles close to phase coexistence, and close to interfacial transitions, is a challenging task.

For $q = 0.5$ and $\Delta = 0.2$ the density functional theory (DFT) predicts fluid-fluid phase separation with a critical point at $\eta_s = 0.049$, $\eta_b = 0.151$—see Fig. 2(b). We start with the b-type wall, which we find does indeed preferentially adsorb the bigger particles. For b-rich state points the preferred species is already at the wall and no surface transitions occur. For s-rich state points at bulk coexistence, but far from the bulk critical point, we find that the small particles dominate the region close to the wall, but that there is a small amount of adsorption of the bigger particles. To illustrate this, see the pair of density profiles $\rho_s(z)$ and $\rho_b(z)$ furthest from the bulk critical point in Fig. 2(a). As η_s is reduced along the binodal in the direction toward the bulk critical point, there occurs a series of discontinuous jumps of the density profiles. The first jump corresponds to the big particles displacing the small particles from the wall and forming a layer at a distance σ_{bb} away from the wall; see Fig. 2(a). Each subsequent jump corresponds to the adsorption of an extra b-rich liquid layer at the wall. Using the coexistence criteria we have located five distinct layering transitions. Beyond the fifth transition we find that the layer rich in the big particles becomes macroscopically thick. We discuss the possible nature of this transition below. The inset to Fig. 2(a) shows the adsorption $\Gamma_i = \int dz\,[\rho_i(z) - \rho_i(\infty)]$, of each species $i = s,b$ as a function of η_s. Each plateau represents the range of state points along the binodal which have a particular number of adsorbed layers. The formation of the infinitely thick layer corresponds to Γ_b jumping to $+\infty$, and Γ_s to $-\infty$. The layering transitions are first-order surface phase transitions, characterized by a range of coexisting states. In Fig. 2(b) we plot the coexistence lines of the first two transitions in the (η_s,η_b) plane. We find that the layering transitions intersect the bulk binodal [13] and that they lie very close to the binodal on the s-rich side of the phase diagram. Each transition terminates at a surface critical point, where the jump in Γ_i vanishes. The first layering transition, where the big particles strongly adsorb at the wall and form the first layer, is the largest both in terms of the change in the adsorptions and in its size on the phase diagram. Each subsequent transition is smaller than the previous one.

We next turn to the s-type wall. As this preferentially adsorbs the smaller particles, tracing the bulk coexistence

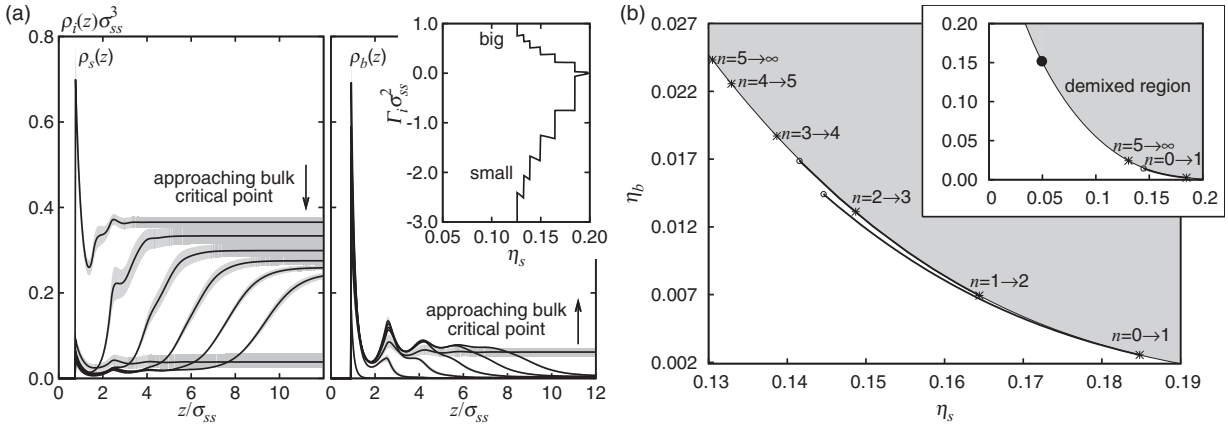

FIG. 2. (a) Pairs of density profiles $\rho_s(z)$ (left panel) and $\rho_b(z)$ (right panel) of the NAHS fluid with $q = 0.5$ and $\Delta = 0.2$ at a b-type wall and at bulk coexistence on the s-rich side of the phase diagram. The shaded regions represent the range of profiles possessing $n = 0$ or 1, 2, 3, 4, or 5 adsorbed b-rich layers, and the region where the adsorbed film becomes infinitely thick. The solid lines represent specific examples from the middle of each range. The inset shows the adsorption of each species Γ_i as a function of η_s. (b) The corresponding phase diagram in the (η_s,η_b) plane. There is a series of layering transitions that intersect the bulk binodal (∗) and descend into the s-rich one-phase region, ending in a surface critical point (○). For clarity only the first two transitions are shown in full, while the remaining transitions are represented only by their intersection with the bulk binodal. The inset shows the location of the first layering and the "wetting" transitions in relation to the bulk critical point (●).

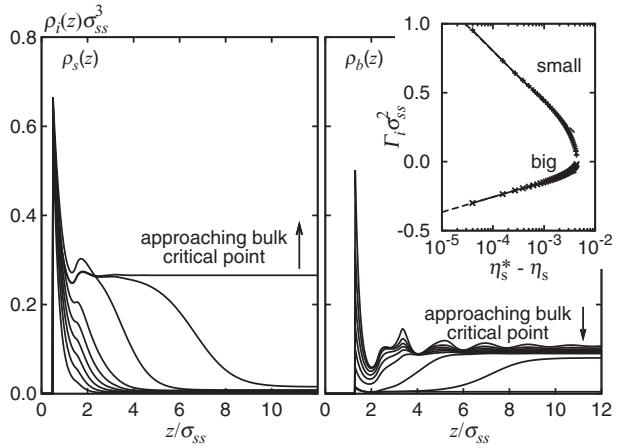

FIG. 3. Same as Fig. 2(a), but for the s-type wall. The coexistence curve is traced on the b-rich side of the phase diagram. As the wetting critical point is approached the smaller particles strongly adsorb at the wall, replacing the bigger particles and growing a thick film. Below the wetting critical point the film is infinitely thick. The inset shows the adsorptions Γ_i against the difference in the packing fraction of the small species from its value at the wetting critical point, $\eta_s^* - \eta_s$, on a logarithmic scale, where $\eta_s^* = 0.0043$.

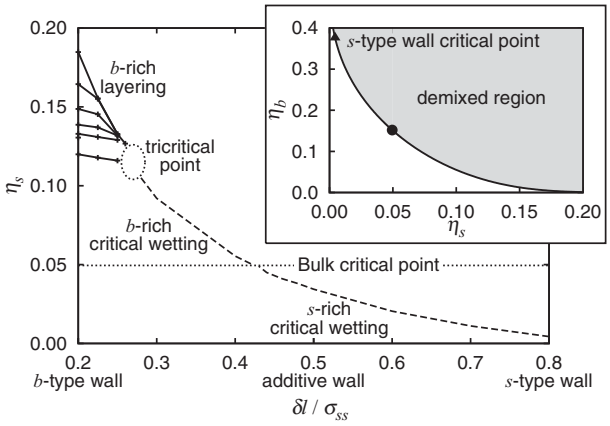

FIG. 4. Value of η_s at (i) the intercept of the layering transitions with the bulk binodal (solid lines) and (ii) the location of the critical wetting transition critical point (dashed line), as a function of the scaled wall offset $\delta l/\sigma_{ss}$. As $\delta l/\sigma_{ss}$ is increased from 0.2 (b-type wall) the layering transitions move along the binodal toward the bulk critical point, located at $\eta_s^{\rm crit} \simeq 0.05$. At $\delta l/\sigma_{ss} \simeq 0.27$ the layering transitions coalesce and the surface transition becomes critical wetting. As δl increases toward the additive case, the critical wetting transition approaches the bulk critical point. Increasing δl further, the wetting critical point moves to the other side of the binodal. The inset shows the s-type wall wetting critical point (▲) in relation to the bulk critical point (●).

curve on its b-rich side is interesting. For state points far from the bulk critical point, we find that there is some adsorption of the small particles, but that big particles dominate the region close to the wall; see the pair of density profiles furthest from the bulk critical point in Fig. 3, where $\rho_b(z)$ exhibits oscillatory decay that indicates high-density packing effects. Increasing η_s along the binodal in the direction of the bulk critical point, we find that the small particles start to adsorb more strongly at the wall, replacing the big particles. On moving further toward the bulk critical point, a thick film rich in the small particles grows. No jumps are observed and the thickness increases continuously (and reversibly) with the state point up to a wetting critical point, beyond which the film is infinitely thick; see Fig. 3. Hence we conclude that this wetting transition is critical. In such a case the adsorption can be shown [14,15] to diverge as $\Gamma_i \propto \ln(|\eta_s^* - \eta_s|)$ on the mean-field level, where η_s^* is the value of η_s at the wetting critical point. We find the value of η_s^* by fitting Γ_i to its asymptotic form. The inset to Fig. 3 compares the adsorptions to the asymptotic logarithmic form. The location of the wetting critical point, $\eta_s^* = 0.0043$, is shown in relation to the bulk binodal in the inset to Fig. 4.

We next vary the wall offset parameter δl between the two cases discussed above. Starting with the b-type wall, $\delta l/\sigma_{ss} = 0.2$, and increasing δl we find that the location of the layering transitions moves toward the bulk critical point. In Fig. 4 we show the value of η_s at each of the intersections of a layering transition and the bulk binodal as a function of δl. The jump in adsorption at each layering transition becomes smaller and the extent of the line in the phase diagram becomes shorter (not shown). Decreasing δl further, we find that at $\delta l/\sigma_{ss} \simeq 0.27$ the individual layering transitions bunch up and become indistinguishable from each other. For smaller δl there is a single continuous wetting transition, where the thickness of the adsorbed b-rich layer grows logarithmically, in a similar manner to the behavior at the s-type wall described above. We establish the location of the surface critical point by fitting Γ_i to its asymptotic form and plot the value of η_s^* at the wetting critical point in Fig. 4. Increasing δl further results in the location of the wetting critical point moving further along the bulk binodal toward the bulk critical point so that at $\delta l/\sigma_{ss} \simeq 0.43$ the wetting transition critical point coincides with the bulk critical point, and the wall is neutral such that neither species is preferentially adsorbed at the wall. As δl is increased beyond 0.43 we find that the wetting transition moves to the b-rich side of the phase diagram. The additive wall, $\delta l/\sigma_{ss} = 0.5$, has a critical wetting transition, but located very close to the bulk critical point. As δl is increased, the wetting critical point moves further along the bulk binodal, so that we return back to the s-type wall, $\delta l/\sigma_{ss} = 0.8$.

In order to ascertain the generality of our findings, we have investigated the trends upon changing the model parameters. For size ratio $q = 0.5$ and vanishing wall offset $\delta l = 0$, we find layering transitions far from the bulk critical point for a range of nonadditivity parameters $\Delta = 0.1, 0.2, 0.5$. As δl is adjusted toward the case of the additive wall, the layering transitions move toward the bulk critical point. We also investigated symmetric mixtures with $q = 1$ and $\Delta = 0.1$. Clearly, for the additive wall, $\delta = 0$, there is no preferential adsorption at the wall and hence no layering transitions. Introducing preferential adsorption via a nonvanishing wall offset, $\delta l = 0.1, 0.2, 0.3$, layering transitions occur, and these move away from the bulk critical point upon increasing δl.

In summary, we have shown that the NAHS model exhibits both layering and critical wetting transitions depending on the hard wall offset parameter. We expect this wetting scenario to be general and to occur in a large variety of systems where

steric exclusion is relevant. A set of layering transitions had been previously found in the AOV model at a hard wall [16]. In these studies the wall parameter is equivalent to the b-type wall. As in these previous papers, the existence of an infinite number of layering transitions is a possibility within our mean-field DFT treatment. The effects of fluctuations would be to smear out the higher-order layering transitions to produce a final wetting transition as found here. A change from a first-order to a critical wetting transition is not uncommon [15]. What is remarkable here is that tricritical behavior can be induced in a purely entropic system by merely changing a nonadditive wall parameter, δl. Moreover, the NAHS model is much less special than the AO model, as here both species (not only the AO colloids) display short-ranged repulsion and hence packing effects. In future work, it would be interesting to see the effects of nonadditivity on wetting in charged systems where first-order and critical wetting transitions occur [5].

We acknowledge funding by EPSRC under Grant No. EP/E06519/1 and by DFG under SFB840/A3.

[1] D. Bonn, J. Eggers, J. Indekeu, J. Meunier, and E. Rolley, Rev. Mod. Phys. **81**, 739 (2009).

[2] J. P. Hansen and I. R. McDonald, *Theory of Simple Liquids*, 3rd ed. (Academic Press, London, 2006).

[3] R. Roth, J. Phys.: Condens. Matter **22**, 063102 (2010).

[4] R. Roth and S. Dietrich, Phys. Rev. E **62**, 6926 (2000).

[5] A. Oleksy and J. P. Hansen, Mol. Phys. **104**, 2871 (2006); **107**, 2609 (2009).

[6] I. Kalcher, D. Horinek, R. Netz, and J. Dzubiella, J. Phys.: Condens. Matter **21**, 424108 (2009); I. Kalcher, J. C. F. Schulz, and J. Dzubiella, Phys. Rev. Lett. **104**, 097802 (2010).

[7] A. Harvey and J. Prausnitz, Fluid Phase Equilib. **48**, 197 (1989); G. Kahl, J. Chem. Phys. **93**, 5105 (1990); L. V. Woodcock, Ind. Eng. Chem. Res. **50**, 227 (2011).

[8] S. Asakura and F. Oosawa, J. Chem. Phys. **22**, 1255 (1954); A. Vrij, Pure Appl. Chem. **48**, 471 (1976).

[9] M. Schmidt, J. Phys.: Condens. Matter **16**, 351 (2004).

[10] P. Hopkins and M. Schmidt, J. Phys.: Condens. Matter **22**, 325108 (2010).

[11] A. Ayadim and S. Amokrane, J. Phys.: Condens. Matter **22**, 035103 (2010).

[12] P. Hopkins and M. Schmidt (unpublished).

[13] For a quantitative comparison of the bulk fluid-fluid demixing phase diagram from DFT and simulations for $q = 0.1$ and 1, see Fig. 3 of Ref. [9] (location of the critical point) and Fig. 4 of Ref. [10] (binodals).

[14] J. Cahn, J. Chem. Phys. **66**, 3667 (1977).

[15] S. Dietrich, in *Phase Transitions and Critical Phenomena*, edited by C. Domb and J. L. Lebowitz (Academic Press, London, 1988), Vol. XII.

[16] J. M. Brader *et al.*, J. Phys.: Condens. Matter **14**, L1 (2002); M. Dijkstra and R. van Roij, Phys. Rev. Lett. **89**, 208303 (2002); P. P. F. Wessels, M. Schmidt, and H. Löwen, J. Phys.: Condens. Matter **16**, S4169 (2004).